Journal of Marine Systems xxx (2013) xxx–xxx

Contents lists available at ScienceDirect

Journal of Marine Systems

journal homepage: www.elsevier.com/locate/jmarsys

Vertical diffusion processes in the Eastern Mediterranean — Black Sea System

Sotiris Kioroglou [a,b,*], Elina Tragou [b], Vassilis Zervakis [b], Dimitris Georgopoulos [a], Barak Herut [d], Isaak Gertman [d], Vedrana Kovacevic [c], Emin Ozsoy [e], Ersin Tutsak [e]

[a] Hellenic Center for Marine Research, Athens Greece
[b] Department of Marine Sciences University of Aegean, Mytilene, Greece
[c] Instituto Nazionale di Oceanografia e di Geofisica Sperimentale, OGS, Italy
[d] Israel Oceanographic and Limnological Research
[e] Institute of Marine Sciences, Technical University of Middle East, Erdemli, Turkey

ARTICLE INFO

Article history:
Received 15 December 2011
Received in revised form 1 August 2013
Accepted 26 August 2013
Available online xxxx

Keywords:
Overturns
Diffusion
Thermohaline staircase
Mixing
Mediterranean
Black Sea

ABSTRACT

The identification and examination of 'complete' potential density overturns in CTD profiles, within the framework of SESAME project, are employed to assess vertical eddy diffusivities, mostly in the top 100 m of the water column, for a broad area covering the East Mediterranean, the Turkish Straits and the Black Sea. The implementation of this method shows that, mixing induced by mechanical turbulence is enhanced in frontal areas, in the proximity of straits and inside anticyclones; furthermore, that mechanical turbulence is insignificant, down to the scale of CTD resolution, within areas of double diffusive staircases, encountered in deep layers of the water column. Consequently, only laminar theories about double diffusion are applied for assessing diffusivities therein. Susceptibility to different types of double diffusion seems to be related to the interaction of different types of water masses.

1. Introduction

Turbulent and/or double diffusive mixing have proven to be significant for physical chemical and biological oceanic processes (e.g., Cullen et al., 1983; Gargett, 1984; Gargett and Holloway, 1984) and their parameterization to play a key role in the effectiveness of numerical models in 'simulating' oceanic processes (McDougall and Ruddick, 1992). In this work we attempt to assess basic parameters of vertical mixing (eddy diffusivities and dissipation rates) for the broader area encompassing the Eastern Mediterranean and the Black Sea, based on CTD data which were acquired within the framework of the EU funded project SESAME. We estimate diffusivities not only for areas characterized solely by mechanical turbulence, but also for areas where double diffusion might be combined with mechanical turbulence.

The 'state of the art' instruments for resolving the full turbulent spectrum, almost down to the Kolmogorov microscale (a few cm), at which turbulence decays due to molecular dissipation, are the vertically free falling (Gregg et al., 1978; Osborn and Crawford, 1980; Wolk et al., 2001) or horizontally towed microprofilers (Mormorino et al., 1987), equipped with fast response vertical shear, temperature and conductivity probes. These have been invented in the seventies and since then are being continually improved and sparsely deployed in the ocean, due to their high cost and requirements for highly specialized personnel.

However vertical profiles of temperature and salinity, (and hence density) that could be valuable for vertical mixing estimates are also provided by standard CTDs, routinely used in oceanographic expeditions since the second half of the 20th century. Admittedly, their resolution and accuracy cannot compete with the data quality provided by a microprofiler. Still, the abundance of available CTD data from the world's oceans and their comparatively low cost acquisition provide a strong motive for exploiting them as a tool for vertical mixing estimates.

The basis of the CTD use in assessing mixing is that turbulence, being three-dimensional, unavoidably results in the 'overturning' of the water column, a situation in which heavier fluid particles lay instantaneously over lighter ones, forming a temporary, statically unstable, Z-shaped configuration in the vertical potential density (σ_θ) profile. We applied the overturn method for areas of pure mechanical turbulence and also for checking whether mechanical turbulence could be combined with double diffusion (Laurent and Schmitt, 1998).

For the second case in particular where mechanical turbulence coexists with double diffusion, laminar theories are not sufficient and modifications accounting for both mixing processes should be implemented (e.g., McDougall and Ruddick, 1992). In this context we first verified that no valid overturns were present within double diffusive areas, before selecting the suitable laminar models for evaluating double diffusive fluxes and diffusivities.

* Corresponding author at: Hellenic Center for Marine Research, PS 16343, 46.7 of Athinon Souniou Avenue, Athens, Greece.
E-mail address: skior@hcmr.gr (S. Kioroglou).

0924-7963/$ – see front matter © 2013 Elsevier B.V. All rights reserved.
http://dx.doi.org/10.1016/j.jmarsys.2013.08.007

This work is divided in 3 sections. In Section 2 we present the spatial and temporal extent of the CTD measurements used in our overturn analysis, in Section 3 we outline the overturn methodology and in Section 4 the results of our data analysis are demonstrated.

2. Spatial and temporal extent of the SESAME CTD measurements

The main goal of the SESAME project was to assess and predict changes in the Mediterranean and Black Sea ecosystems as well as changes in the ability of these ecosystems to provide goods and services. Many participating countries simultaneously launched oceanographic cruises at selected areas, in an effort to conduct both standard and specialized oceanographic measurements over a station grid extending from Gibraltar Strait, Otranto Strait and Ionian Sea, Southeast Mediterranean, through the Aegean Sea, to the Turkish Straits and the Black Sea.

We hereby analyze CTD data of the East Mediterranean branch of the experimental area (Fig. 1). The CTD data profiles, extending through the whole water column, were acquired by four marine research centers, OGS of Italy, HCMR of Greece, IMS-METU of Turkey, and IOLR of Israel, at a sampling rate of $R = 24$ Hz, providing a vertical depth resolution $r = R / w = 3$–5 cm where w is the CTD descent rate, ranging from 0.7 m/s to 1 m/s. Within the framework of this work, no vertical averaging was performed on the data apart from the standard quality control, so that the structural details of the profile of the potential density could be maximized. Each research center participating in SESAME was assigned a specific area survey to be conducted simultaneously with surveys of the rest of the participating research centers, such that the whole Mediterranean and Black Seas were covered by an extensive grid of oceanographic stations. In an attempt to assess seasonal variability, the stations of the grid were sampled in winter 2008 and in summer 2008, during two different oceanographic cruises, hereafter referred to as SES1 and SES2, respectively. Moreover two additional separate cruises (winter 2008, summer 2008) were conducted right at the aftermath of the two major aforementioned seasonal cruises, at the two seas connected by the strait of Dardanelles, i.e., the North Aegean Sea and the Sea of Marmara. The purpose of the latter cruises was to study the modification and interaction processes of the Black Sea and the East Mediterranean waters along their route (Lagrangian experiments) from the Black Sea into the north Aegean (the area in Fig. 1 below enclosed by an ellipse). The CTD data of these separate cruises are also encompassed within the scope of our analysis.

3. The overturn methodology

The initial step of the data analysis, preceding the overturn identification, was the standard CTD data processing towards eliminating systematic errors such as the ones induced by the short term mismatch of the temperature and conductivity sensor responses or the thermal lag of the conductivity cell (Lueck and Picklo, 1990; Morison et al., 1994). Both of these effects result in spikes that 'contaminate' the data profiles with 'apparent' overturns. Data corresponding to depth reversals were also excluded as probable contaminants, by keeping only records with pressure larger than all the previous records of the profile (Stansfield et al, 2001).

Furthermore, we developed an algorithm identifying the vertical boundaries of complete overturns. Complete overturns are local mixing patches, enclosing the motions of all fluid parcels inside them. They constitute vertical turbulent areas that are distinctly separated from 'calm' waters above and below them. Our whole analysis has been based on the identification of these patches whereby the attribute 'complete' has been omitted for brevity. Within overturn patches fluid parcels are temporarily displaced from their stable positions. The Thorpe displacements L_{Ti} from unstable to stable positions within a complete overturn are known to sum up to zero, i.e., it is valid that $\sum_{i=1}^{i=\eta} L_{Ti} = 0$ due to the conservation of total mass. This relation in discrete form was implemented as a criterion of identifying the complete overturn boundaries in the aforementioned algorithm.

The subsequent quality control of the identified overturns, consisted of an implementation of the methodology initially developed by Galbraith and Kelley (1996), as modified by Johnson and Garrett (2004), towards isolating artifacts from systematic errors, like salinity spikes and instrument noise.

As a matter of fact Galbraith and Kelley (1996) were the first to devise a comprehensive pair of criteria, for distinguishing 'real' from 'apparent' overturns caused by systematic errors and noise respectively.

Their so called 'water mass' criterion addressing the systematic errors, is based on the hypothesis that the data depicting an overturn correspond to the same water mass, both before (stable regime) and after (unstable regime) the overturn creation. Consequently the unstable temperature and salinity values should be well correlated within a real overturn. This criterion expressed mathematically, imposes that two 'water mass' numbers, ξ_T, ξ_S, representing the degree of smooth covariance of temperature and salinity versus density respectively, be less than a threshold value of 0.5 (see Section 1.1 of online supplement). We used a more 'generous' threshold value of 1, counterbalancing this generosity with careful visual inspection of each overturn we identified.

As to testing 'noisy' overturns, the Galbraith and Kelley (1996) criterion regards as 'noisy' the overturns that practically have on average very small 'run lengths', where a run-length is the number of adjacent unstable points within an overturn that will have to move in the same direction (upwards or downwards), towards their stable positions.

This criterion is opposed to noise free overturns with sufficiently large signal to noise ratio, characterized by large run-lengths, induced by the approximate 'Z' unstable shape of their density profiles. Indeed, the Z shape is consistent with top (heavier, overlying) fluid parcels moving downwards, forming a large run, and bottom (lighter, underlying) fluid parcels moving downwards forming a second large run.

Johnson and Garrett (2004) showed however that the Galbraith run-length criterion is both too strict (rejects some real overturns as results of noise) and insufficient in correctly discerning 'real' from 'noisy' overturns. They further suggested an improved noise criterion, where one considers a linear model of the potential density profile of the overturn area and 'superimposes' on it random noise of amplitude equal to the profile instrument's noise amplitude. Discerning between 'noisy' and 'real' overturns is then based on the comparison between

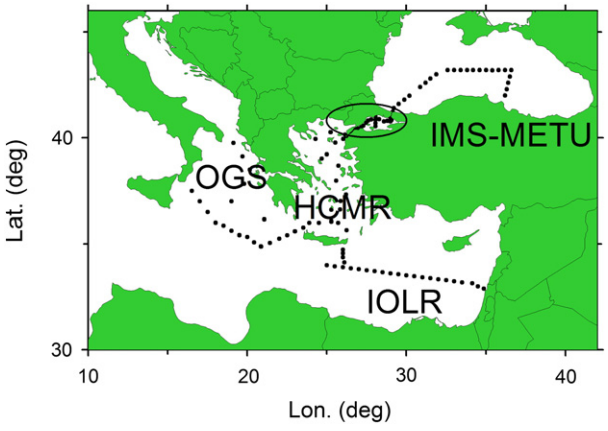

Fig. 1. The grid of oceanographic stations of SESAME2 branch in East Mediterranean and Black Sea.

Please cite this article as: Kioroglou, S., et al., Vertical diffusion processes in the Eastern Mediterranean — Black Sea System, J. Mar. Syst. (2013), http://dx.doi.org/10.1016/j.jmarsys.2013.08.007

run-lengths and Thorpe scales of the 'measured' and the 'noise-modeled' overturns (see Section 1.2 of online supplement).

Within the framework of this study, the above-mentioned quality control has been implemented but also extended towards locating density overturns induced by CTD motion induced by the ship's heaving and rolling. A detailed description of the developed methodology to identify and reject such overturns, is described in Section 1 of the online supplement.

A quality control of identified overturns, according to the previously analyzed tests, was also implemented to layers and interfaces of double diffusive areas. We were motivated by the fact that the identification of 'real' overturns within these areas could enable the calculation of 'total' diffusivities according to the McDougall and Ruddick (1992) approach, applied in areas where both double diffusion and mechanical turbulence produce mixing (Laurent and Schmitt, 1998).

Finally, having identified 'real' overturns, we further assessed turbulent mixing parameters, as follows.

The so called Thorpe scale, L_T, was first estimated on the basis of density profiles (Thorpe, 1977). It is defined as the rms value of the Thorpe displacements L_{Ti}, which are the displacements of the fluid particles from their unstable to their stable positions. The key factor enabling turbulence estimations based on CTD induced L_{Ti} values, is the correlation between L_{Ti} and the Ozmidov scale L_0, defined as

$$L_0 = \left({}^{\varepsilon}/_{N^3}\right)^{1}/_{2} \quad (1)$$

where ε is the dissipation rate of kinetic energy, and N is the buoyancy frequency. Dillon (1982) showed that on average,

$$L_T \approx 0.8 L_0 \quad (2)$$

which enables the calculation of ε, if the values of N and L_T are specified by use of CTD data. Furthermore, a Fickian (equal to property flux/property vertical gradient) mass eddy diffusivity, K_ρ, can be estimated as shown by Osborn (1980), according to

$$K_\rho = \frac{\Gamma \varepsilon}{N^2}, \quad (3)$$

where Γ is a mixing efficiency coefficient approximately equal to 0.2.

4. Results

4.1. Time and space variability of overturning

The selected as 'real' overturns were used in our analysis, for evaluating dissipation rates and diffusivities of mechanical turbulence given by Eqs. 1 to 3. Fig. 2 shows histograms of populations of various parameter values characterizing the overturns, separately for each of the two cruises (time variability) as well as for various areas (spatial variability). The populations are much larger for almost all the values in SES2. This could be partly attributed to the better weather conditions during the late summer SES2 experiments, allowing for more CTD stations to be conducted.

An additional reason of the SES2 stations, presenting more overturns, could be the relatively less frequent 'contamination' of the CTD's vertical motion by the rolling motion of the ship. This is expected to be analogous to the degree of weather adversity.

Indeed, in harsher weather conditions, the ship-motion is more likely to cause variations in the CTD's descent rate, which might appear in the form of overturns in the profile, as explained in Section 2 of the online supplement. Our method just identifies and discards these overturns. Among them, however, there might be certain cases, where ship-motion-induced, contaminate real seawater overturns. It is rather impossible to reliably extract the ship-motion-induced part and accept the residual part as real overturn. Thus, the 'resultant' overturn appears to be ship-motion-induced and gets discarded as a whole. The discards are expected to be more in heavier weather resulting in a bias towards the accepted as 'real' overturns being more in good weather conditions.

Dissipation rate and diffusivity peak at $10^{-9.5}$ W/Kg, $10^{-4.5}$ m^2 s^{-1} in winter and 10^{-9} W/Kg, 10^{-5} m^2 s^{-1} in summer, respectively. There appears to exist no difference with respect to vertical background potential density gradient N^2, which peaks at 10^{-5} s^{-2}in both seasons, the most frequent values ranging from $10^{-5.5}$ to 10^{-4} s^{-2}.

Most overturns occurred within the top 20 m in winter (SES1), and in the 20 m to 40 m layer during summer (SES2) and quite a few also occurred in the 40 m to 80 m layer.

As to the spatial variability of overturn occurrence, four spatial categories have been distinguished, i.e., the Aegean Sea, the Black Sea, the Ionian Sea and the East Mediterranean. The histograms peak at the abovementioned values and it is notable that most overturns have occurred in the Marmara Sea (shown as part of the 'Black Sea' group) and the North Aegean (part of the Aegean group). These are the areas of the Marmara–North Aegean system where the 'core' water masses of the Black Sea (fresh and cold) and the Mediterranean (warm and salty) intermingle and mix. The south, central Aegean and Ionian overturn populations on the other side, are also pronounced, but smaller than the ones of the North Aegean–Marmara system.

In particular, the Ionian Sea upper layer is classified as an area of intense vertical mixing between the 'fresh' and cold surface water of Atlantic origin (Modified Atlantic Water, MAW), Ionian Surface Water (ISW, during summer clearly discerned from MAW, by being saltier and warmer (Manca et al., 2006)) and the saline and warm subsurface water of the East Mediterranean (Levantine Intermediate Water, LIW). All these water masses and principal pathways have been thoroughly analyzed by Malanotte-Rizzoli et al. (1997).

Moreover, mesoscale dynamic structures that populate the Ionian Sea, such as multi-lobe anticyclones, endorse the entrainment and interaction therein of LIW water masses produced in different years and therefore characterized by different residence times, TS properties and equilibrium depths. This interaction, expressed in the form of mechanical mixing, occurs in a vertically broader regime and could be the driving agent of the aforementioned Ionian overturns detected at depths of 200 m.

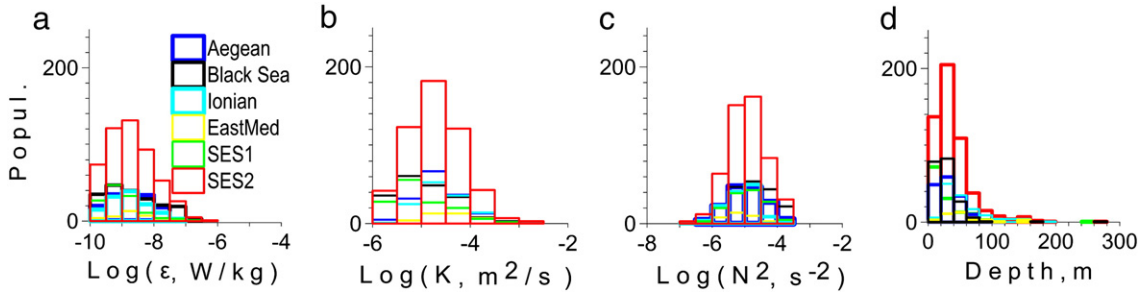

Fig. 2. Histograms of log-scaled dissipation rate ε, diffusivity K, squared Brunt Väisala frequency N^2 and depth of overturn centroid for the overturns. Temporal (SES1, SES2) and spatial (Aegean Sea, Black Sea, Ionian Sea and East Mediterranean) dependence.

Please cite this article as: Kioroglou, S., et al., Vertical diffusion processes in the Eastern Mediterranean — Black Sea System, J. Mar. Syst. (2013), http://dx.doi.org/10.1016/j.jmarsys.2013.08.007

More specifically, a dominant mechanism of the aforementioned mechanical mixing of the water column, expected to occur at the subsurface areas where different water masses intermingle, is that of the Kelvin–Helmholtz instability occurring when 'destabilizing' shear overcomes (by being at least 4 times larger) the stabilizing stratification, resulting in values of low (less than ¼) Richardson number (Miles, 1961). This instability seems to be correlated with the strain intensity of isopycnic surfaces (Alford and Pinkel, 2000; Kunze et al., 2006) and also be enhanced by the incidence of trapped, near inertial, internal waves inside anticyclonic eddies. The 200 m deep overturns seen in the histograms of the Ionian probably fall in the category of anticyclonic shear intensification whereas the ones of the Sea of Marmara could be attributed to a combination of hydraulically controlled shear intensification and strain enhancement induced by nonlinear wave–wave interactions.

The aforementioned results seem to agree with the results of BOUM oceanographic cruise, conducted within the framework of SESAME in summer 2008 (see Cuypers et al., 2012), studying vertical mixing rates along a transect extending all the way along the Mediterranean Sea. In their work, dissipation rates were inferred both directly by microstructure measurements within anticyclonic eddies and indirectly, using fine scale parameterization of shear and N^2 based on CTD and LADCP fine scale data, following Gregg (1989), appropriately modified to account for strain to shear ratio, following Polzin et al. (1995).

In particular, for 3 sampled anticyclonic eddies along a section extending from the West to East Mediterranean, they derived dissipation rates of the order of 10^{-8}–10^{-7} W/Kg, in the pycnocline region between 10 and 20 m depth, and $<10^{-9}$ W/Kg below 20 m down to 100 m. The diffusivity values ranged from 5×10^{-5} m^2 s^{-1} to 1×10^{-5} m^2 s^{-1} in the two aforementioned depth extents respectively. Fig. 3 below confirms the general agreement between our work and the work by Cuypers et al. (2012). Focusing on the red data points, corresponding to SESAME2 Ionian–East Mediterranean data, as to the ones being temporally and spatially most related to the BOUM data, we note that the agreement is evident in the value range of the overlaid dashed segment representing a linear regression over the Ionian–East Mediterranean section data of SESAME2, depicting a gradual decrease from 10^{-7} W/Kg at 10–20 m to 10^{-10} W/Kg at 100 m. The larger dispersion values of our data compared to the BOUM values can be attributed to the sporadic distribution of overturn locations over our CTD deployments, as contrasted to the BOUM data values corresponding to averaging over dissipation rates at specific depths over an ensemble of complete microstructure profiles. For the same reason our diffusivity values do follow a more sporadic depth distribution ranging from 10^{-5} m^2 s^{-1} to 10^{-4} m^2 s^{-1}, although they are in general agreement with the corresponding BOUM data.

In order to obtain a more detailed insight of the time and space variability of the overturns, we studied their distribution during both cruises SES1 and SES2, along two different vertical sections, S1 and S2, encompassing the whole study area (Fig. 4), thus producing 4 transects, hereafter referred to as SES1_S1, SES1_S2, SES2_S1 and SES2_S2. Transects SES1_S1 and SES2_S1 span the area from Otranto Strait in the North Ionian Sea, through the western Cretan Arc Straits into the Aegean Sea, through the Dardanelles Strait into the Sea of Marmara, through the Bosporus strait into the Black Sea. Sections SES1_S2 and SES2_S2 extend from the pelagic area east of Sicily, through the south Ionian Sea, through the Cretan passage south of the Greek island of Crete, to the eastern extreme of the Mediterranean, the coasts of the Middle East. The transects show overturn diffusivities overlaid on salinity temperature and σ_θ (potential density) for the top 400 m of the water column.

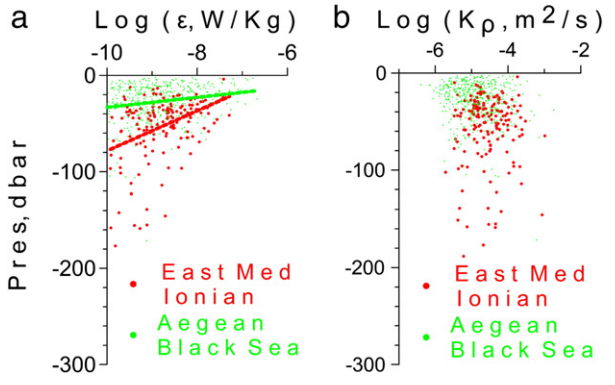

Fig. 3. Dissipation rates (left) and vertical eddy diffusivities (right), derived with the overturn method, as functions of depth for the East Mediterranean–Ionian and Aegean–Black Sea areas.

Proceeding with our description along the sections from west to east and from south to north we attempt to relate the overturn frequency of appearance and mixing intensity with the local hydrodynamic conditions. In this context the S1 and S2 sections will be referred to, in terms of the geographic areas they traverse and the cruise season as SES1,2_S1, Ionian, South Aegean, North Aegean, Turkish Straits and Black Sea and SES1,2_S2, Ionian, Cretan Passage, Levantine-East Mediterranean extreme, respectively.

As to the Ionian SES1_S1, there are 4 overturns at the flanks of a major anticyclone, labeled as O1 to O4, where shear might be the dominant factor in temporarily overturning the water. The deepest overturn, O4, at 230 m, is located near the geographic extreme of the isopycnals, which coincides with the anticyclonic center. The overturning might be relatively more frequent at the peripheries of cyclones or anticyclones, because these areas might favor diapycnal instabilities induced by the ever decreasing value of the stratification to shear ratio (the so called gradient Richardson number) as we move away from these centers, along the isopycnals. A possible scenario might be the following: as the curvature of the anticyclonic or cyclonic isopycnals near their geographic extremes (troughs, peaks) changes fast, the horizontal and vertical distances between any two specific isopycnals increases as we move along the isopycnals away from the cyclonic or anticyclonic vortices. This in turn results in vertical density gradients (stratification) becoming progressively smaller and vertical gradients of horizontal velocity (shear) becoming progressively larger (due to the thermal wind equations). Thus, internal waves with propagation axis forming a small angle with the isopycnals, could be subjected to an increasingly unstable environment, and the interaction of the wave motion with the anticyclonic or cyclonic motion might result in wave breaking and overturning. Moreover, in anticyclonic areas in particular, shear could get intensified due to the presence of trapped, near inertial internal waves (Kunze, 1985; Kunze, 1995). A very large fraction of the overturns of all 4 sections can be classified as belonging to the aforementioned categories (additionally to the already mentioned overturns, also O5, O6, O7, O8 and O9 of section SES2_S1, O10 and O11 of SES1_S2 and O12, O13, O14 and O15 of SES2_S2).

The Ionian SES1_S1 region seems to be less diapycnally diffusive than the SES2_S1 one. During SES2, a lot of overturns were recorded at station IT_1, at the proximity of the Otranto strait, in a vertical section extending down to the depth of 70 m. Vertical mixing is expected to intensify near straits, where the flow and shear are also intensified due to hydraulic controls like constrictions and sills (Gregg, 2004), and these shears could be advected downstream by the mean flow.

In the Ionian SES2_S1, near station I10, a set of overturns, shown encircled by a blue ellipse in Fig. 4, are located at the boundary of a fresh anomaly, forming a blue vertically elongated lens, within more saline (green color) background, extending from 50 m to 100 m. This fresh anomaly is a signature of the MAW, which spreads from the Strait of Sicily towards the Eastern Mediterranean and the Ionian Sea. Similar features of the low salinity lenses, as well as a presence of multi-lobe anti-cyclonic eddies have been encountered and described also by Malanotte-Rizzoli et al. (1999). More recent observations, in 2007, also present such dynamic features (Kovačević et al., 2012)

Please cite this article as: Kioroglou, S., et al., Vertical diffusion processes in the Eastern Mediterranean — Black Sea System, J. Mar. Syst. (2013), http://dx.doi.org/10.1016/j.jmarsys.2013.08.007

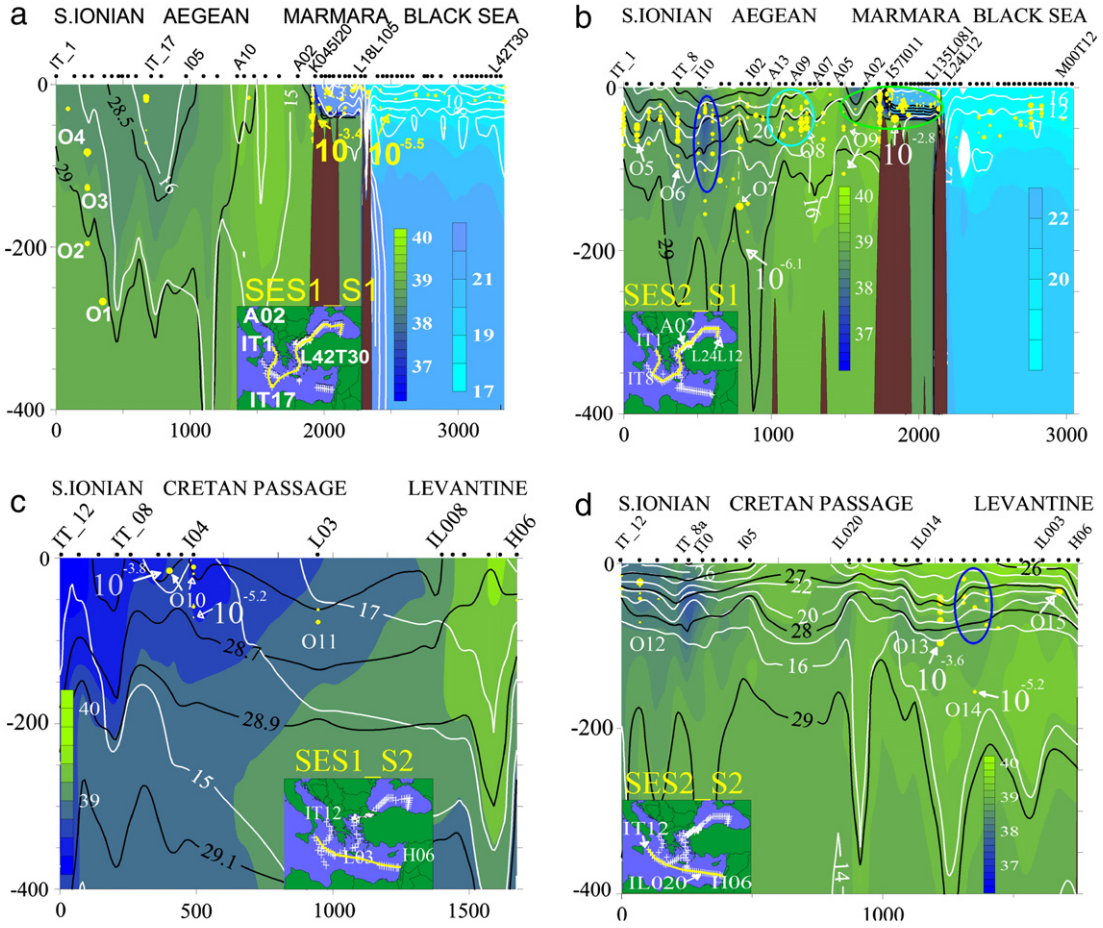

Fig. 4. Transects S1 (top) and S2 (bottom) of SES1 (left) and SES2 (right) cruises of the 400 top meters of the water column. The transects show the salinity in color scale along with the θ (white) and σ_θ (black) contours. Especially for the salinity distributions of the S1 (top), 2 different color scales have been used, for depicting equally well the salinity stratifications of both the EastMed–Aegean area and the Black Sea–Marmara area, two totally hydrologically different but communicating areas. The sharp transfer from the saline Aegean waters to the Marmara brackish waters of Black Sea origin is achieved chromatically as a transfer from blue to cyan. The white gaps correspond to very low salinity values, not included in the Black Sea color scale representing the 'bulk' salinity values. The yellow filled circles are log scaled diffusivities, and 2 diffusivity values are shown in each transect for 'visualizing' the scale. The inlaid maps show with yellow lines the sections under consideration; the crosses in them show the CTD stations. On top of each of the 4 panels there are shown names of some of the CTD stations and the names of corresponding geographic areas, and the filled black circles on top of the panes show the locations of the CTD stations along the section.

constituting examples of mixing between different water masses, aided by overturning of the water column. Other example cases of overturning in areas where water masses of different characteristics intermingle is the North Aegean–Turkish Straits system, shown encircled by the green ellipse in the SES2S1 transect of Fig. 4, and a less pronounced case is the set of overturns that is shown encircled by a blue ellipse in the SES2S2 transect, located in the south branch of the Levantine between stations IL014 and IL003.

At this point we note additionally that almost all overturns are located inside the seasonal thermocline, such a case being the SES2S1 overturns near Sicily (station IT_12). Inside the thermocline, due to the enhanced stratification, more energy is required to trigger overturns than in mixed layers. On the other side, however, it is easier to detect such overturns due to their high signal to noise ratio, while the intense mixing within the surface mixed layer would remain undetectable by the current method, due to the density homogeneity. The signal is indeed high within the thermocline because the potential density gradient is large, thus one can resolve density differences over smaller vertical extents without exceeding the instrumental noise limits.

In the south Aegean during SES1, only a few CTD casts have been deployed and only one overturn identified, in station A10 of transect SES1_S2, due to adverse weather conditions. During SES2 (transect SES2_S1) in turn, overturns have been identified both in the south and north Aegean. The south Aegean stations A13 to A9, encircled by the cyan ellipse in Fig. 4, cover the stretch from the western Cretan arc straits (A13) to the eastern Cretan sea (A9). This is one of the major areas of communication between the Aegean Sea and the East Mediterranean (Balopoulos et al, 1999; Kontoyiannis et al., 1999; Zodiatis, 1992a; Zodiatis, 1993a; Zodiatis, 1993b) and of outflow of the Cretan Dense Water (CDW), that filled the deepest layers of the East Mediterranean in the early 1990s (Theocharis et al., 1999).

The aforementioned SES2_S1 overturns of the south Aegean occupy the layer extending from 50 m to 100 m, in contrast to the north Aegean ones (stations A5, A7, and A2) that occupy the entire upper 100 m layer of the water column. The north Aegean overturns are related to intense local mixing between water masses of quite different origin and characteristics, i.e., of the brackish Black Sea Water (BSW), filling the top 20 to 30 m of the water column, exiting from the Dardanelles Strait into the North Aegean, and the underlying Levantine Water (LW), originated from the Levantine area of the East Mediterranean (see also Zervakis and Georgopoulos, 2002; Zodiatis and Balopoulos, 1993). The major mixing area between the two water masses is encircled by the green ellipse in section SES2_S1 of Fig. 4. It encompasses the northeast Aegean Sea, the Marmara Sea and the western shelf of the Black Sea and the straits of Dardanelles and Bosphorus, connecting the Marmara Sea to the Aegean and Black Seas respectively.

As to the Marmara Sea, overturning is distributed throughout the top 70 m of the water column during winter (SES1), the most intense occurring in the proximity of the straits of Dardanelles (near station K045120) and Bosphorus (near station L18L105), due to the hydraulically

Please cite this article as: Kioroglou, S., et al., Vertical diffusion processes in the Eastern Mediterranean — Black Sea System, J. Mar. Syst. (2013), http://dx.doi.org/10.1016/j.jmarsys.2013.08.007

controlled intensification of flow (Gregg and Özsoy, 2002; Kanarska and Maderich, 2008; Oguz, 2005). Also, there is intense mixing at the top 30 m throughout the horizontal extent of the Marmara part, because of winter weather conditions. In comparison, during summer (SES2) overturning is still intense at the proximity of the two straits, but also weaker in the internal Marmara area, especially at the top 30 to 40 m, due to the calmer weather conditions and higher stratification (late summer).

Proceeding to the Black Sea, we note that the overturns occur at shallower depths (0–40 m) during winter (SES1) than during summer (SES2). During winter all overturns are located above the Cold Intermediate Layer (CIL). This is a layer spanning the depth range from 50 m to 100 m, filled with a distinctly cold water mass (core temperature of about 6.5 °C), the so called Cold Intermediate Water (CIW), formed during cold winters, either at the NW Black Sea shelf (Tolmazin, 1985) or in the central Black Sea cyclones (Ovchininikov and Popov, 1987) and further horizontally advected; it acts as the main inhibitor of diapycnal diffusion at larger depths (see also Özsoy and Ünlüata (1997) for a general review about the Black Sea). Remarkably though, during summer, the bulk of overturning activity has been recorded within and immediately below the CIL (Fig. 5 below), and could be attributed to enhanced shear between the CIL and the deeper layer. Özsoy and Ünlüata (1997) suggest that the interaction of CIW with inflowing LIW off the mouth of Bosphorus at the Black Sea side, caused by the temporal lifting of the LIW stream (due to a sill) at the CIW level, is the main agent of the formation of a heavier (colder) mass that sinks further downwards from the shelf edge, causing double diffusive lateral intrusions along and during its descent. The sill off the Bosporus entrance is a region of hydraulically imposed intensified mechanical intermingling of the two masses, and the hereby observed overturns in the region might be originated there and advected horizontally within the CIL layer by the mean flow.

In the North Aegean Sea overturns have been identified at station A1, located at approximately the same latitude as the Dardanelles and in proximal stations that took place in the framework of the two Lagrangian experiments mentioned in Section 2.

4.2. Overturning in the Dardanelles outflow current in the North Aegean

Two Lagrangian experiments were conducted in the North Aegean by HCMR and the Department of Marine Sciences of the University of Aegean at the aftermath of the major SESAME cruises, SES1, SES2. Their main objective was to study the environmental and biochemical transformation of the BSW water mass along its path after leaving the Dardanelles Strait and entering the Aegean (Frangoulis, 2010).

Satellite SST images were used for approximately mapping the core BSW upon its exit from the Dardanelles; more detailed mapping of sea-surface temperature and salinity was produced locally through thermosalinograph survey routes, in order to locate core BSW through its salinity minimum signature. Lagrangian drifters were then deployed within the core, in combination with a drifting sediment trap. CTD/rosette and zooplankton net casts as well as primary production experiments were held along the Lagrangian track of the drifters. Concurrently with the HCMR/University of the Aegean cruises in the North Aegean, IMS-METU conducted regular oceanographic surveys in the Marmara Sea. Throughout the data sets produced by these surveys, most of the overturns were identified at the BSW depth extent, where there is a sharp temperature salinity and potential density gradient between the core BSW and the underlying top layer of LW at approximately 70 m. The source of these overturns could either be Kelvin–Helmholtz instabilities (Miles, 1961) occurring at the interface between the two water masses, or internal wave breaking processes.

Regarding the quantification of the latter process, Gargett and Holloway (1984) examined the dependence of vertical eddy diffusivity on the local buoyancy frequency (N), and derived a general relation,

$$K = \alpha N^q \tag{4}$$

where α is a site specific coefficient depending on the internal wave energy level, and q ranges at values from -1, corresponding to nearly monochromatic waves, to the value of $-1/2$, corresponding to the broad band oceanic internal wave spectrum GM79 (Munk, 1981). Although (4) is expected to hold mostly in the open ocean, away from

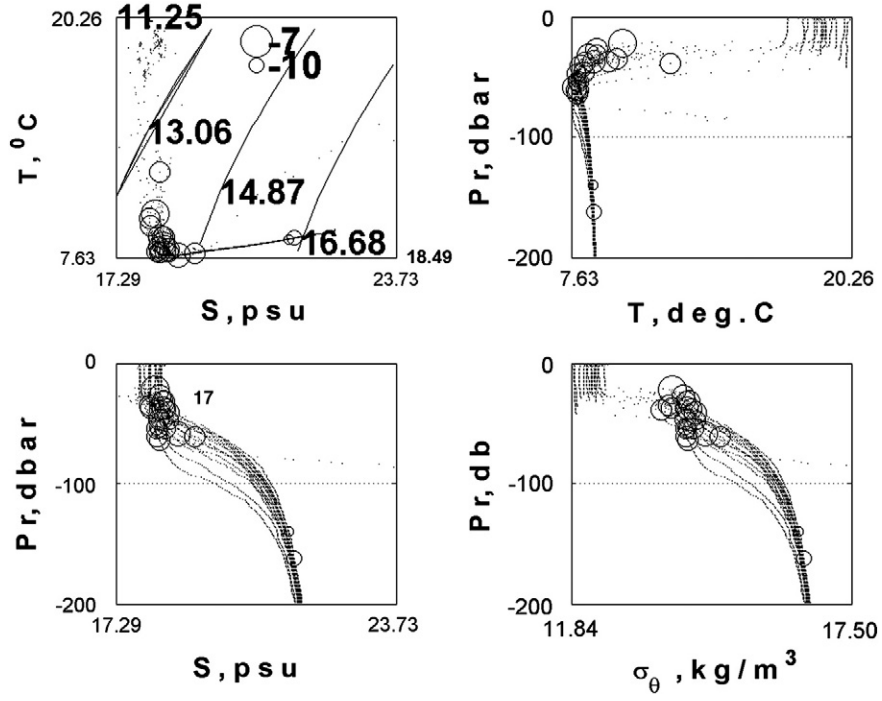

Fig. 5. Distribution of Black Sea overturns versus the properties of the water column. The overturns are represented by the intensity of the 'Thorpe-derived' dissipation rates, shown as log-scaled circles. Top left: temperature (T)–Salinity (S) diagram. Top right: temperature versus pressure (P). Bottom left: Salinity versus pressure. Bottom right: Potential density anomaly (Sth) versus pressure.

Please cite this article as: Kioroglou, S., et al., Vertical diffusion processes in the Eastern Mediterranean — Black Sea System, J. Mar. Syst. (2013), http://dx.doi.org/10.1016/j.jmarsys.2013.08.007

boundary mixing, we tried to assess its applicability for the North Aegean–Marmara Sea system.

Fig. 6 shows K versus N for the SES1, SES2 cruises in the North Aegean and Marmara Seas. The solid lines are best fits to the data and the dotted and dashed lines correspond to formula (4) for single frequency ($q = -1$) and for a broad band of frequencies ($q = -1/2$) respectively. In particular, we set the condition that the two latter lines have the same intercept, choosing an intercept value resulting in lines that 'enclose' the majority of the data set as tightly as possible. The intercept corresponds to α of formula (4), i.e., the energy of the internal wave spectrum. Since α relates to the amount of the local internal wave energy, the requirement that α have the same value for the two extreme cases, is equivalent with the local internal wave energy amount being the same for both cases of single frequency and broad band spectrum internal waves, which makes sense for a specific area with short time and space scales. We can clearly see that the only line of best fit, reasonably agreeing with the values of $\alpha = 10^{-7}$ and $q = -1$, appropriate for the ocean (Gargett and Holloway, 1984) is the one corresponding to the North Aegean Lagrangian data set, the best fit log(intercept) (−7.9) and slope (1.2) estimations being characterized by a determination coefficient $R^2 = 0.30$ and resulting in $K = 10^{-7.9} N^{-1.2}$. In all other cases the best fit lines are not in agreement with (4); this fact suggests that maybe the dominant overturn generation process in the regions of interest is not internal wave breaking, but possibly vertical shear instabilities. In any case, the 'extreme' lines seem to bound tightly the majority of the data points in all four cruises, with SES1 (Winter) values of log(intercept) −6.95 (north Aegean) and −6.8 (Marmara) and SES2 (Autumn) values of log(intercept) −6.5 (north Aegean) and −6.65 (Marmara). Therefore, although the study area is very variable dynamically, we could derive the following approximate 'bounding' equations for the system of North Aegean and Sea of Marmara,

$$K = 10^{-6.9} N^{-1}, K = 10^{-6.9} N^{-1/2}, \quad (5)$$

for the winter and

$$K = 10^{-6.6} N^{-1}, K = 10^{-6.6} N^{-1/2} \quad (6)$$

for the summer–autumn conditions.

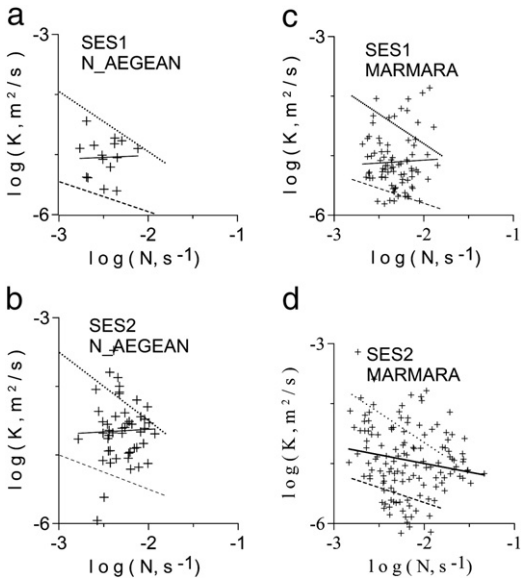

Fig. 6. Log–log plots of diffusivity K versus buoyancy frequency N for the Lagrangian experiments in North Aegean and the corresponding synchronous experiments in the Marmara Sea.

4.3. Double diffusion in EastMed and Black Sea

Both eastern Mediterranean and Black Seas are characterized by large vertical extents of the deep water column where both temperature and salinity vertical gradients, T_z, S_z share the same sign (Kelley et al, 2003; Onken and Brambilla, 2003; Tait and Howe, 1971; Zodiatis and Gasparini, 1996). This is the major condition favoring the emergence of double diffusive structures appearing as vertical sequences of alternatively positioned 'layers', with vertically homogeneous T and S and 'interfaces', with sharply changing T and S within them. These sequences are called 'thermohaline staircases' and are categorized as 'diffusive layers' (henceforth referred to as 'dl') if 'background' T and S both increase with depth, or 'salt fingers' (henceforth referred to as 'sf') if T and S both decrease with depth.

The development of staircases under double diffusion requires relatively stable and laminar environments (found even in thermohaline lenses, or water mass intrusions) (Armi et al, 1989; Zodiatis, 1992b). Several models predicting double diffusive fluxes and diffusivities in such environments have been developed (Kelley, 1984; Kelley, 1990; Kunze, 1987). However, in cases where mechanical turbulence coexists with double diffusion, the laminar theory has to be modified to account for both turbulent and double diffusive mixing processes (e.g., McDougall and Ruddick, 1992). Under this scope it is essential to primarily examine whether or not mechanical turbulence emerges within double diffusive areas before selecting the suitable theoretical model for evaluating fluxes.

In this study, in order to examine whether mechanical turbulence is the dominant mixing process, the layers and interfaces of staircases were identified as separate mixing areas and tested according to the overturn criteria outlined in Section 3.

In particular, potential temperature (θ) and salinity (S) profiles of the SES1 and SES2 cruises were plotted in 100 m segments, and all step-like structures were assembled and categorized according to type ('dl' or 'sf'). Not a single overturn satisfying our validity criteria was identified within these layers and/or interfaces. Therefore all staircases were treated as laminar, according to either 'dl' (Kelley, 1984, 1990) or 'sf' (Kunze, 1987) and the length-scales of these layers and interfaces were used for assessing associated fluxes and diffusivities.

Fig. 7 shows samples of step-like intrusions and staircases from different areas of the eastern Mediterranean and Black Seas. The first from left (SES2_Ionian station IT6_1a) and fifth from left (SES2_Marmara station, K354J184) panels present intrusions, surrounded by double diffusive staircases of both types ('sf', 'dl'). At these two stations, 'dl' stairs are observed at the upper branches of the intrusions and 'sf' stairs at the lower branches (two intrusions, at 210 m and 230 m, in S2_IT6_1a, one intrusion in S2_K354J184 at 60–80 m). These staircases exhibit θ and S gradients of the same signs, positive at the upper branches (favoring 'dl' types) and negative at the lower ones, favoring 'sf' types (Rudels et al., 2009).

The second from left panel shows a large, deep 'sf' staircase, (spanning a depth extent from 700 m to 1000 m) at the proximity of the Levantine in the EastMed, where both temperature and salinity decrease with depth due to the transition from 'hot' and 'saline' Levantine Intermediate Water at the top to relatively fresher and colder water under it.

The third and fourth from left panels correspond to 'sf' diffusive staircases inside the Aegean. In particular, the staircase of SES1 station A3a, located at the depth extent from 500 m to 600 m is expected to be hydrologically and geographically isolated, as A3a is located within the Skyros deep Basin of the North Aegean and its waters of depth more than 300 m do not communicate with the neighboring deep basins, due to the 300 m deep surrounding shelves. Dense waters formed during deep and dry winters in the North and Central Aegean might get advected to the area of Skyros basin, convected to their equilibrium depths and practically remain stagnant in the isolated deep basins (Zervakis et al., 2000; Zervakis et al., 2003). These

Please cite this article as: Kioroglou, S., et al., Vertical diffusion processes in the Eastern Mediterranean — Black Sea System, J. Mar. Syst. (2013), http://dx.doi.org/10.1016/j.jmarsys.2013.08.007

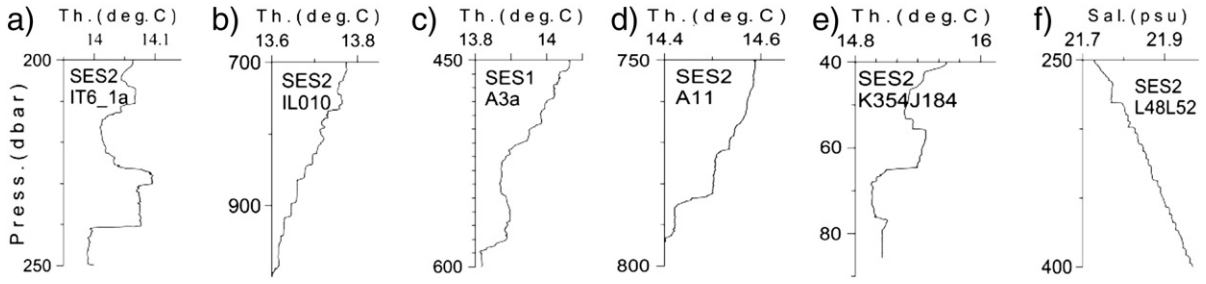

Fig. 7. Double diffusive staircases in the East Mediterranean and Black Sea.

conditions favor the formation of 'laminar' 'sf' staircases such as the one of station S1_A3a. The 'sf' staircase of S2_A11 (750 m to 800 m) is located inside the deep Cretan Sea, under the equilibrium depth of salty and hot LIW spreading.

Finally, the SES2 station L48L52 'dl' staircase of the 6th panel from left, extending from 250 m to 400 m, lies inside the Black Sea.

As becomes evident, depending on their vertical hydrological structure, various portions of the water column are 'susceptible' to different double diffusion types i.e., to 'sf' or 'dl' type. Additionally, the hydrological conditions might result to 'stability' or 'instability'. The criterion is quantified by the value range of the so called Turner angle, *Tu*, (Ruddick, 1983), defined as

$$Tu = -\operatorname{arctg}\left(\frac{\alpha^{\partial T}/_{\partial z}}{\beta^{\partial S}/_{\partial z}} + 45\right) \tag{7}$$

where α and β are the coefficients of thermal expansion and haline contraction of seawater respectively.

The vertical area under consideration is classified as 'dl', 'sf', stable or unstable, if $-90° < Tu < -45°$, $45° < Tu < 90°$, $|Tu| > 90°$, $-45° < Tu < 45°$ respectively (Zodiatis and Gasparini, 1996). We evaluated *Tu* values along sections, SES1_S1, SES1_S2, SES2_S1, SES2_S2, by applying (7) on the CTD data and implementing a suitable interpolation scheme on our estimations.

Fig. 8 shows the *Tu* and double diffusive diffusivities values along the aforementioned transects. In the Ionian SES1_S1 transect, extending from Otranto Strait (station IT1) to south Ionian (stations IT17, I05), the portion of the water column from 200 m to 1000 m is 'sf' susceptible, almost continuously. This structure is attributed to the hot and saline LIW waters filling the Ionian from 200 to 400 m at various places, vertically mixing with less saline and colder waters beneath. From 1000 m to the bottom the column is mostly stable, interrupted by 'sf' and 'dl' susceptible patches in alternating order, caused by intrusions (mostly at station I05). The above observations agree with previous analysis of Zodiatis (1992b).

In fact, the LIW induced 'sf' susceptibility is a common feature throughout the portion of SES1_S1 from Otranto Strait in the north Ionian to Marmara Sea, at the subsurface layer from approximately

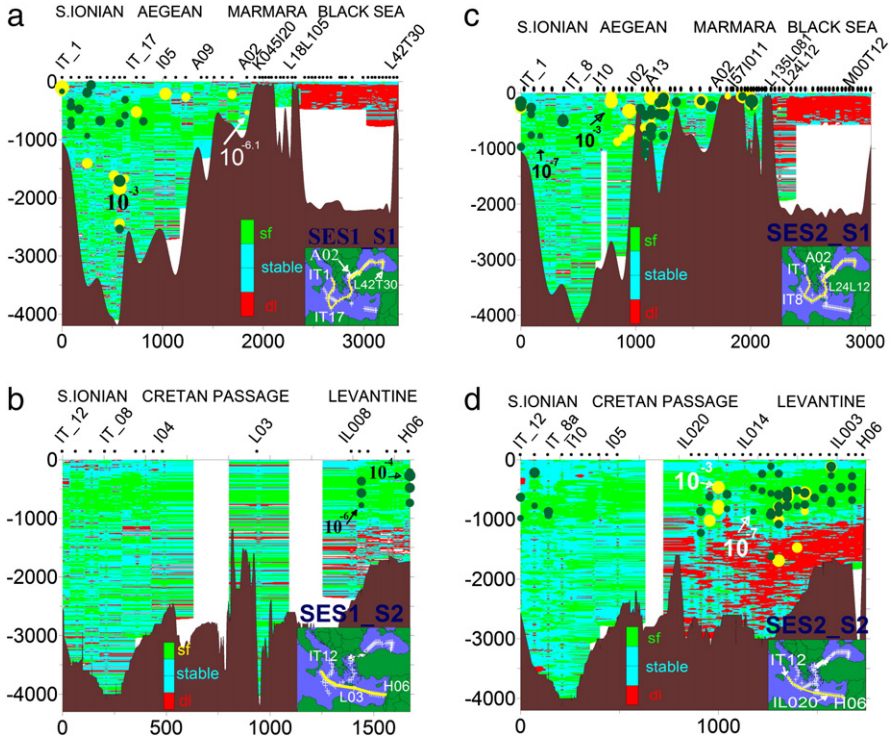

Fig. 8. Transects S1 (top) and S2 (bottom) of SES1 (left) and SES2 (right) cruises showing the spatial distribution of Turner angle and diffusivities of 'dl' and 'sf' type. The vertical multicolored columns indicate unstable, 'sf' susceptible and 'dl' susceptible double diffusion. The circles show double diffusive, apparent mass diffusivities in common log scale. In particular, the filled circles show log scaled diffusivities of 'sf' (forest green) or 'dl' (yellow) types, averaged over the vertical extent of the corresponding thermohaline staircases. In the inlaid maps, the yellow lines show the routes along the sections under consideration and the white crosses show the locations of the CTD stations. On top of each of the 4 panels there are shown names of some of the CTD stations, the CTD locations (by the filled black circles) and the corresponding geographic areas. (For interpretation of the references to color in this figure legend, the reader is referred to the web version of this article.)

Please cite this article as: Kioroglou, S., et al., Vertical diffusion processes in the Eastern Mediterranean — Black Sea System, J. Mar. Syst. (2013), http://dx.doi.org/10.1016/j.jmarsys.2013.08.007

50 m or more to approximately 800 m, where the LIW water mass prevails. This structure is interrupted by either 'dl' patches induced by cold and fresh intrusions, or by stable patches. Exceptionally, in the North Aegean and Marmara Seas the surface 50 to 100 m are 'dl' structured due to the local prevalence of the surface Black Sea Water (BSW), inducing a vertical transition from cold and brackish (BSW) to the hot and saline waters of the underlying upper branch of LIW waters. Finally, we underline the almost thorough 'dl' susceptibility structure of the top 500 m of the Black Sea part of SES1_S1 (the CTD stations were only 500 m deep during SES1), interrupted intermittently by stable patches. As a matter of fact the whole water column of BSW is known to be 'dl' susceptible, from top to bottom, which is facilitated by the warm, saline Mediterranean water intruding from the Bosphorus, cascading down the continental slope and horizontally intruding on its way to filling the bottom waters (Kelley et al., 2003; Özsoy and Ünlüata, 1997).

A more comprehensive view of the double diffusive processes rises from its statistics: To that purpose, diffusivity histograms and depth distribution are presented in Fig. 9. It is clear that the 'sf' events 'dominate' in terms of population at the 100 to 1000 m column, in all of Ionian, Aegean and EastMed, with diffusivities ranging mostly between 10^{-6} and 10^{-4} m^2 s^{-1}. The 'dl' events prevail both in intensity and population at large depths (>1000 m) in all 3 areas, reaching depths of 2500 m and diffusivities of 10^{-4}, 10^{-3} m^2 s^{-1}. Additionally, intense 'dl' events (characterized by diffusivities of 10^{-3} m^2 s^{-1}) occur at the top 500 m, mostly in North Aegean and Marmara – Black Sea, as already shown.

Conclusively, for each of the examination areas, i.e., for the Ionian Sea, the Aegean Sea, the eastern Mediterranean, and the Marmara Sea–Black Sea system, we averaged over all included staircases, for deriving mean stability ratios, R_ρ, flux ratios, and diffusivities of Temperature, Salinity and mass, all shown in following Table 1. The stability ratios range from 1 to 2 for most of the areas. For the 'sf' events this means large 'sf' growth rate (Laurent and Schmitt, 1998), while for the 'dl' events, it does mean increasing uncertainty in the formulas used to predict fluxes (Kelley, 1984; Kelley, 1990). Prominent 'dl' exception is the Black Sea – Marmara system, being characterized by a large stability ratio, equal to 12, for which the theory predicts more accurately fluxes and diffusivities. The mean buoyancy flux ratios, γ, are rather well within the range that the 'dl', 'sf' theories predict. Finally we conclude that the 'dl' diffusivities are on average (10^{-4} to 10^{-3} m^2 s^{-1}), i.e. an order of magnitude larger than the 'sf' diffusivities (10^{-7} to 10^{-4} $m^2 s^{-1}$).

5. Conclusions

In this work the vertical diffusion processes in the eastern Mediterranean and Black Seas were quantified and mapped at large scale. Both turbulent and double diffusive mixing estimates were produced.

The identification and examination of potential density overturns was used as means for estimating vertical eddy (turbulent) diffusivities, in the East Mediterranean and the Black Sea, based purely on CTD data. This method is mostly successful in areas of significant density gradients, such as the seasonal thermocline. However it might be successful in distinguishing 'real' overturns from noise in deeper regimes. In areas lacking observable overturns, double diffusion theory was applied to produce diffusivity estimates either due to salt fingering or diffusive layering.

Most turbulent overturning is recorded within the top 100 m of the water column. It emerges in the proximity of strait areas, the Otranto Strait, and the Turkish straits, where hydraulic enhancement of the exchange flow and shear seems to be the driving process of overturning of the water column. Many overturns are also identified at the periphery of anticyclonic meanderings where vertical shear is enhanced. Overturning appears to be more intense in areas of vertical mixing between different water masses, such as between Black Sea Water and Levantine Water in the Turkish Straits–North Aegean–West shelf of the Black Sea area, or next to the Otranto Strait in North Ionian.

Double diffusive fluxes based on laminar theories were estimated at regions where no significant (to the CTD resolution limits) turbulent overturning was identified within the deep thermohaline staircases. The susceptibility to different types of double diffusion appears to be correlated to the relative vertical position of different water masses;

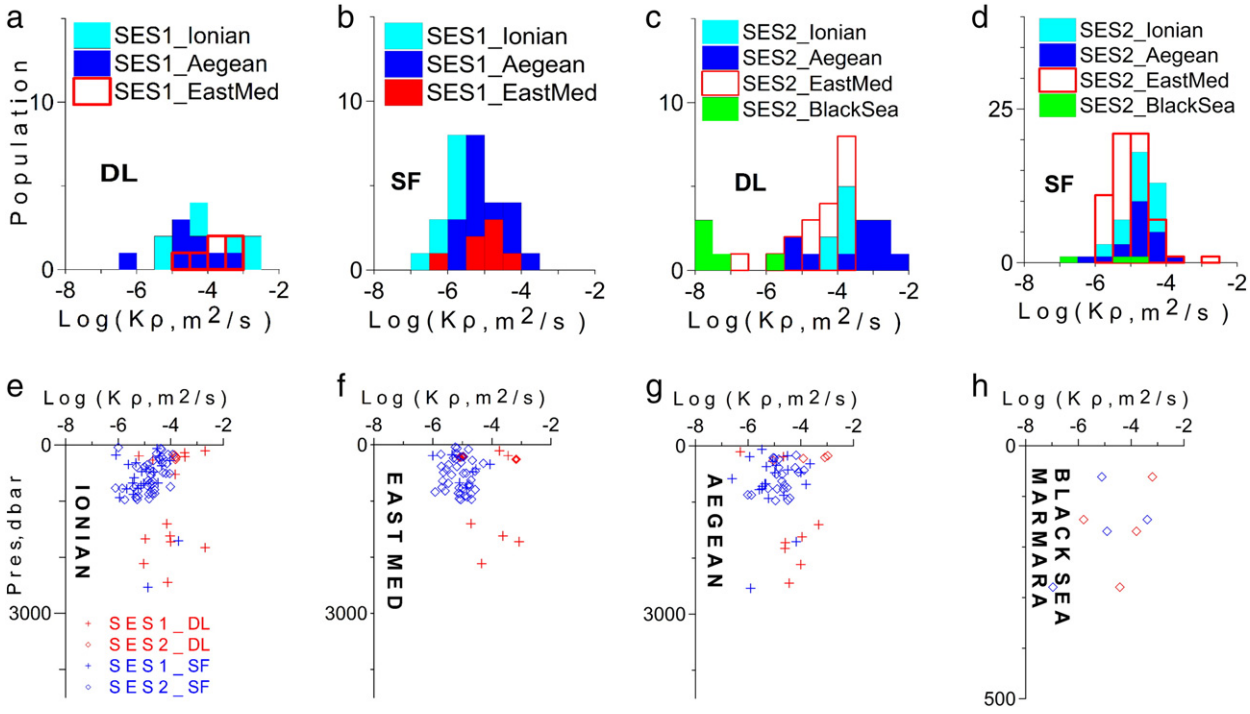

Fig. 9. Histograms of double diffusive 'apparent' diffusivity of mass, K_ρ, for SES1 SES2 cruises (top) and depths of K_ρ for Ionian, eastern Mediterranean, Aegean and Black Sea–Marmara areas respectively (bottom).

Please cite this article as: Kioroglou, S., et al., Vertical diffusion processes in the Eastern Mediterranean — Black Sea System, J. Mar. Syst. (2013), http://dx.doi.org/10.1016/j.jmarsys.2013.08.007

Table 1
Mean double diffusion parameters per area (Ionian, Aegean, EastMed, Black Sea Marmara) and per season (SES1, SES2).

	R_ρ	γ	Log(K_T)	Log(K_S)	Log(K_ρ)
SF					
Ses1_Ionian	2.7 ± 2.0	0.6 ± 0.1	−6.2 ± 0.6	−5.5 ± 0.9	−5.0 ± 0.6
Ses2_Ionian	1.4 ± 0.7	0.6 ± 0.1	−6.2 ± 0.6	−5.1 ± 0.8	−4.8 ± 0.5
Ses1_Aegean	1.2 ± 0.4	0.6 ± 0.1	−6.1 ± 0.7	−4.9 ± 1.1	−4.9 ± 0.6
Ses2_Aegean	2.0 ± 0.3	1.5 ± 0.3	−5.2 ± 0.5	−4.8 ± 0.8	−7.4 ± 0.5
Ses1_EastMed	1.7 ± 0.9	0.6 ± 0.1	−6.2 ± 0.7	−5.4 ± 0.9	−5 ± 0.7
Ses2_EastMed	1.5 ± 0.3	0.7 ± 0.1	−6.2 ± 0.6	−5.6 ± 0.7	−5 ± 0.5
DL					
Ses1_Ionian	1.3 ± 0.6	0.4 ± 0.2	−5.1 ± 0.6	−5.6 ± 0.8	−4 ± 0.7
Ses2_Ionian	1.0 ± 0.6	0.5 ± 0.2	−5.0 ± 0.1	−5.4 ± 0.2	−3.0 ± 0.0
Ses1_Aegean	1.5 ± 0.7	0.5 ± 0.2	−5.4 ± 0.8	−5.9 ± 0.8	−4.0 ± 0.7
Ses2_Aegean	1.4 ± 0.6	0.5 ± 0.2	−4.9 ± 0.7	−5.9 ± 0.2	−3.9 ± 1.0
Ses1_EastMed	1.1 ± 0.4	0.5 ± 0.2	−4.8 ± 0.4	−5.2 ± 0.5	−3.8 ± 0.6
Ses2_EastMed	1.1 ± 0.7	0.6 ± 0.3	−4.8 ± 0.8	−5.3 ± 0.8	−3.8 ± 0.9
Ses2_BlackSea	12.6 ± 16	0.3 ± 0.2	−5.8 ± 1.2	−7.1 ± 2	−5.3 ± 2

different basins and areas exhibit inclination to either salt fingering or double diffusive layering. Following the various turbulence-free double diffusive models applied, the identified double diffusion coefficients are 1 to 3 orders magnitude less than the 'overturning' diffusivities of the top 100 m of the water column.

The method can be applied on historical studies of vertical diffusion too, since there is a wealth of CTD data since the 1950s. Nevertheless the results prove that more detailed mixing studies should be conducted in the East Mediterranean - Black Sea system, focused mostly on the time and space variability of overturning and on the stability types of the water column. Comparative studies between CTD and microstructure profiler measurements could assist in further improving the contribution of CTD profiles to assessment of vertical eddy diffusivities. The recent developments of combining microstructure measurements with the use of autonomous underwater vehicles and oceanographic gliders may constitute the turning point for the provision of high quality, high-volume data shedding light to the mixing processes in the southern European Seas.

Acknowledgments

We would like to express our gratitude to the crews, the officers and the participating scientists and technicians during the SESAME cruises of the 4 research vessels of Italy, Greece, Turkey, and Israel. We would also like to thank the anonymous reviewers whose suggestions helped to improve this work.

This work has been conducted within the framework of the project 'Southern European Seas: Assessing and Modeling Ecosystem changes (SESAME)', funded by the European Union's sixth Framework Programme (FP6), under the priority 'Sustainable Development, Global Change and Ecosystems', contract no. GOCE-2006-036949.

Appendix A. Supplementary data

The following is the Supplementary data to this article.SUPPLEMENT_ONLINE_Kioroglou et_al_vertical_diffusion_process…vised.doc.

Appendix A. Supplementary data

Supplementary data to this article can be found online at http://dx.doi.org/10.1016/j.jmarsys.2013.08.007.

References

Alford, M.H., Pinkel, R., 2000. Observations of overturning in the thermocline: the context of ocean mixing. J. Phys. Oceanogr. 30, 805–832.

Armi, L., Hebert, D., Oakey, N., Price, J.F., Richardson, P.L., Rossby, H.T., Ruddick, B., 1989. Two years in the life of a Mediterranean Salt Lens. J. Phys. Oceanogr. 19, 354–370.

Balopoulos, E.Th., Theocharis, A., Kontoyiannis, H., Varnavas, S., Voutsinou-Taliadouri, F., Iona, A., Souvermezoglou, A., Ignatiades, L., Gotsis-Skretas, O., Pavlidou, a., 1999. Major advances in the oceanography of the southern Aegean Sea–Cretan Straits system (eastern Mediterranean). Prog. Oceanogr. 44, 109–130.

Cullen, J.J., Stewart, E., Renger, E., Eppley, R.W., Winnant, C.D., 1983. Vertical motion of the thermocline, nitracline and chlorophyll maximum layers in relation to currents on Southern Californian Shelf. J. Mar. Res. 41, 239–262.

Cuypers, Y., Bouruet-Aubertot, P., Marec, C., Fuda, J.L., 2012. Characterization of turbulence from a fine-scale parameterization and microstructure measurements in the Mediterranean Sea during the BOUM experiment. Biogeosciences 9, 3131–3149. http://dx.doi.org/10.5194/bg-9-3131-2012 (www.biogeosciences.net/9/3131/2012/).

Dillon, T.M., 1982. Vertical overturns: a comparison of Thorpe and Ozmidov length scales. J. Geophys. Res. 87, 9601–9613.

Frangoulis, C., 2010. Connecting export fluxes to plankton food-web efficiency in the Black Sea waters inflowing into the Mediterranean Sea. J. Plankton Res. 32, 1203–1216.

Galbraith, P.S., Kelley, D.E., 1996. Identifying overturns in CTD Profiles. J. Atmos. Ocean. Technol. 13, 688–702.

Gargett, A.E., 1984. Vertical diffusivity in the ocean interior. J. Mar. Res. 42, 359–393.

Gargett, A.E., Holloway, G., 1984. Dissipation and diffusion by internal wave breaking. J. Mar. Res. 42, 15–27.

Gregg, M.C., 1989. Scaling turbulent dissipation in the thermocline. J. Geophys. Res. 94, 9686–9698.

Gregg, M.C., 2004. Small scale processes in straits. Deep-Sea Res. II 51, 489–503.

Gregg, M.C., Özsoy, E., 2002. Flow, water mass changes and dynamics in the Bosphorus. J. Geophys. Res. 107 (C3), 3016. http://dx.doi.org/10.1029/2000JC000485.

Gregg, M.C., Meagher, T.B., Pederson, A.M., Aagaard, E.A., 1978. Low noise temperature microstructure measurements with thermistors. Deep-Sea Res. 25, 843–856.

Johnson, H.L., Garrett, C., 2004. Effects of noise on Thorpe scales and run lengths. J. Phys. Oceanogr. 34, 2359–2371.

Kanarska, Y., Maderich, V., 2008. Modelling of seasonal exchange flows through the Dardanelles Strait. Estuar. Coast. Shelf Res. 79, 449–458.

Kelley, D.E., 1984. Effective diffusivities within oceanic thermohaline staircases. J. Geophys. Res. 89, 10484–10488.

Kelley, D.E., 1990. Fluxes through diffusive staircases: a new formulation. J. Geophys. Res. 95, 3365–3371.

Kelley, D.E., Fernando, H.J.S., Gargett, A.E., Tanny, J., zsoy, E., 2003. The diffusive regime of double-diffusive convection. Prog. Oceanogr. 56, 461–481.

Kontoyiannis, H., Theocharis, A., Balopoulos, E., Kioroglou, S., Papadopoulos, V., Collins, M., Velegrakis, A.F., Iona, A., 1999. Water fluxes through the Cretan Arc Straits, Eastern Mediterranean Sea: March 1994 to June 1995. Prog. Oceanogr. 44, 511–529.

Kovačević, V., Manca, B.B., Ursella, L., Schroeder, K., Cozzi, S., Burca, M., Mauri, E., Gerin, R., Notarstefano, G., Deponte, D., 2012. Water mass properties and dynamic conditions of the Eastern Mediterranean in June 2007. Prog. Oceanogr. 104, 59–79 (http://dx.doi.org/10.1016/j.pocean.2012.05.006).

Kunze, E., 1985. Near-inertial wave propagation in geostrophic shear. J. Phys. Oceanogr. 14, 544–565.

Kunze, E., 1987. Limits on growing, finite-length salt fingers: a Richardson number constraint. J. Mar. Res. 45, 533–556.

Kunze, E., 1995. The energy balance in a warm core ring's near inertial critical layer. J. Phys. Oceanogr. 25, 942–957.

Kunze, E., Firing, E., Hummo, J.M., Chereskin, T.K., Thurnherr, A.M., 2006. Global abyssal mixing inferred from lowered ADCP shear and CTD strain profiles. J. Phys. Oceanogr. 36, 1553–1576.

Laurent, L.S., Schmitt, R.W., 1998. The contribution of salt fingers to vertical mixing in the North Atlantic Tracer Release Experiment. J. Phys. Oceanogr. 29, 1404–1424.

Lueck, R.G., Picklo, J.J., 1990. Thermal inertia of conductivity cells: observations with a Sea-Bird cell. J. Atmos. Ocean. Technol. 7, 756–768.

Malanotte-Rizzoli, P., Manca, B.B., D'Alcala, M.R., Theocharis, A., Bergamasco, A., Bregant, D., Budillon, G., Civitarese, G., Georgopoulos, D., Michelato, A., Sansone, E., Scarazzato, P., Souvermezoglou, E., 1997. A synthesis of the Ionian Sea hydrography, circulation and water mass pathways during POEM-Phase I. Prog. Oceanogr. 39, 153–204.

Malanotte-Rizzoli, P., Manca, B.B., D'Alcala, M.R., Theocharis, A., Brenner, S., Budillon, G., Ozsoy, E., 1999. The Eastern Mediterranean in the 80s and in the 90s: the big transition in the intermediate and deep circulations. Dyn. Atmos. Oceans 29, 365–395.

Manca, B.B., Ibello, V., Pacciavoni, M., Scarazzato, P., Giorgetti, A., 2006. Ventilation of deep waters in the Adriatic and Ionian Seas following changes in the thermohaline circulation of Eastern Mediterranean. Clim. Res. 31, 239–256.

McDougall, T.J., Ruddick, B.R., 1992. The use of ocean microstructure to quantify both turbulent mixing and salt fingering. Deep-Sea Res. 39, 1931–1952.

Miles, J.W., 1961. On the stability of heterogenous flows. J. Fluid Mech. 10, 496–508.

Morison, J., Anderson, R., Larson, N., D'Asaro, E., Boyd, T., 1994. The correction for thermal—lag effects in Sea-Bird CTD data. J. Atmos. Ocean. Technol. 11, 1151–1164.

Mormorino, Brown, Gl O.W.K., Morris, W.D., 1987. Two dimensional temperature structure in the C-SALT thermohaline staircase. Deep-Sea Res. 34, 1667–1676.

Munk, W.H., 1981. Internal Waves and Small-scale Processes. Evolution of Physical Oceanography. In: Warren, B.A., Wunsch, C. (Eds.), MIT Press, pp. 264–290.

Oguz, T., 2005. Hydraulic adjustments of the Bosphorus exchange flow. Geophys. Res. Lett. 32, L06604. http://dx.doi.org/10.1029/2005GL022353.

Onken, R., Brambilla, E., 2003. Double diffusion in the Mediterranean Sea: observation and parameterization of salt finger convection. J. Geophys. Res. 108, 8124–8136.

Osborn, T.R., 1980. Estimates of the local rate of vertical diffusion from dissipation measurements. J. Phys. Oceanogr. 10, 83–89.

Osborn, T.R., Crawford, W.R., 1980. An Airfoil Probe for Measuring Velocity Fluctuations in Water. Air–Sea Interaction: Instruments and Methods. In: Dobson, F., Hasse, L., Davis, R. (Eds.), Plenum, N.Y. (801 pp.).
Ovchininikov, I.M., Popov, Yu.I., 1987. Evolution of the cold intermediate layer in the Black Sea. Oceanology 27, 555–560.
Özsoy, E., Ünlüata, Ü., 1997. Oceanography of the Black Sea: a review of some recent results. Earth-Sci. Rev. 42, 231–272.
Polzin, K.L., Toole, J.M., Schmitt, R.W., 1995. Finescale parameterizations of turbulent dissipation. J. Phys. Oceanogr. 25, 306–328.
Ruddick, B., 1983. A practical indicator of the stability of the water column to double diffusive activity. Deep-Sea Res. 30, 1105–1107.
Rudels, B., Kuzmina, N., Shauer, U., Tapani, S., Zhurbas, V., 2009. Double-diffusive convection and interleaving in the Arctic Ocean — distribution and importance. Geophysica 45, 199–213.
Stansfield, K., Garett, C., Dewey, R., 2001. The probability distribution of the Thorpe displacement within overturns in Juan de Fuca Strait. J. Phys. Oceanogr. 31 (I), 3421–3434.
Tait, R.I., Howe, M.R., 1971. Thermohaline staircase. Nature 231, 178–179.
Theocharis, A., Balopoulos, E., Kioroglou, S., Kontoyiannis, H., Iona, A., 1999. A synthesis of the circulation and hydrography of South Aegean Sea and the Straits of the Cretan Arc. Prog. Oceanogr. 44, 469–509.
Thorpe, S., 1977. Turbulence and mixing in a Scottish loch. Philos. Trans. R. Soc. Lond. 286A, 125–181.
Tolmazin, D., 1985. Changing coastal oceanography of the Black Sea I. Northwestern Shelf. Prog. Oceanogr. 15, 277–316.
Wolk, F., Yamazaki, H., Seuront, L., Lueck, R.G., 2001. A new free fall profiler for measuring bio-physical microstructure. J. Atmos. Ocean. Technol. 19, 780–793.
Zervakis, V., Georgopoulos, D., 2002. Hydrology and circulation in the North Aegean (Eastern Mediterranean) throughout 1997 and 1998. Mediterr. Mar. Sci. 3, 5–19.
Zervakis, V., Georgopoulos, D., Drakopoulos, P.G., 2000. The role of the North Aegean Sea in triggering the recent Eastern Mediterranean climatic changes. J. Geophys. Res. 105, 26103–26116.
Zervakis, V., Krassakopoulou, E., Georgopoulos, D., Souvermezoglou, E., 2003. Vertical diffusion and oxygen consumption during stagnation periods in the deep North Aegean. Deep-Sea Res. I 50, 53–71.
Zodiatis, G.M., 1992a. On the seasonal variability of the water masses circulation in the NW Levantine–Cretan Sea and flow through the eastern Cretan Arc Straits. Ann. Geophys. 10, 12–24.
Zodiatis, G.M., 1992b. Lens formation in the SE Ionian Sea and double diffusion. Ann. Geophys. 10, 935–942.
Zodiatis, G.M., 1993a. Circulation of the Cretan Sea water masses (Eastern Mediterranean Sea). Oceanol. Acta 16 (2), 107–114.
Zodiatis, G.M., 1993b. Water mass circulation between the SE Ionian–W Cretan basins through the western Cretan arc straits. Bolletino di Oceanologia Teorica ed Applicata XI (No 1), 61–75.
Zodiatis, G.M., Balopoulos, E., 1993. Structure and characteristics of Fronts in the North Aegean Sea. Bolletino di Oceanologia Teorica ed Applicata XI (No.2), 113–124.
Zodiatis, G.M., Gasparini, G.P., 1996. Thermohaline staircase formations in the Tyrrhenian Sea. Deep-Sea Res. 43, 655–678.

Please cite this article as: Kioroglou, S., et al., Vertical diffusion processes in the Eastern Mediterranean — Black Sea System, J. Mar. Syst. (2013), http://dx.doi.org/10.1016/j.jmarsys.2013.08.007